Dose profile monitoring with carbon ions by means of prompt-gamma measurements

Etienne Testa, M. Bajard, M. Chevallier, Denis Dauvergne, Fabrice Le Foulher, Nicolas Freud, Jean Michel Létang, J.-C. Poizat, Cédric Ray, Mauro Testa

Dose profile monitoring with carbon ions by means of prompt-gamma measurements

E. Testa[1], M. Bajard[1], M. Chevallier[1], D. Dauvergne[1], F. Le Foulher[1], N. Freud[2], J.M. Létang[2], J.C. Poizat[1], C. Ray[1], M. Testa[1]

[1]Institut de Physique Nucléaire de Lyon, Université de Lyon, F-69003 Lyon; Université Lyon 1 and IN2P3/CNRS, UMR 5822, F-69622 Villeurbanne, France

[2]Institut National des Sciences Appliquées de Lyon, Laboratoire de Contrôle Non-Destructif par Rayonnements Ionisants

Abstract

A key point in the quality control of ion therapy is real-time monitoring and imaging of the dose delivered to the patient. Among the possible signals that can be used to make such a monitoring, prompt gamma-rays issued from nuclear fragmentation are possible candidates, provided the correlation between the emission profile and the primary beam range can be established. By means of simultaneous energy and time of flight discrimination, we could measure the longitudinal profile of the prompt gamma-rays emitted by 73 MeV/u carbon ions stopping inside a PMMA target. This technique allowed us to minimize the shielding against neutrons and scattered gamma rays, and to find a good correlation between the prompt gamma profile and the ion range. This profile was studied as a function of the observation angle. By extrapolating our results to higher energies and realistic detection efficiencies, we showed that prompt gamma-ray measurements make it feasible to control in real time the longitudinal dose during ion therapy treatments.

PACS: 29.20_C; 21.60.Ka; 29.20.Hm

Keywords: hadrontherapy; dosimetry; monitoring; prompt gamma-rays;

I. Introduction

Hadrontherapy is a radiation therapy modality with proton or light ion beams that presents two main advantages over conventional radiotherapy techniques: a much better physical dose conformation to tumor volumes and a Relative Biological Efficiency (RBE) that is close to unity along the main part of the ion track (in healthy tissue) and typically of the order of 2 or 3 at the Bragg peak location (that corresponds to a position inside the tumor). These two advantages make hadrontherapy particularly indicated for the treatment of radioresistant tumors [1].

Such an accuracy and efficiency require the precise verification of the dose distribution delivered to the patient. Indeed, contrary to photons, the maximum dose is deposited at the Bragg peak location that depends strongly on the beam parameters and on the nature of the traversed tissues. The tissues may be strongly heterogeneous and varying with time. Other difficulties to obtain the matching between the treatment planning and the dose delivered arise from the high precision required for the patient positioning on the treatment couch and patient or organ movement.

The methods of dose monitoring during hadrontherapy treatment are based on the γ-ray emission following the nuclear reactions undergone by some incident ions. The fraction of incident ions which fragment before stopping in tissues is about 15% at 100 MeV/u and 70% at 400 MeV/u [2]. The current systems of control used in Germany and Japan use the technique of Positron Emission Tomography (PET) that measures the annihilation location of

β+ particles emitted by the radionuclides activated during irradiation [3]. Two methods are possible: in-beam PET that allows *in-situ* therapy control (with beam and patient positioning restrictions) or off-line PET with commercial ring tomography. However, the β^+-activity induced by hadron irradiation is relatively low, which implies that the PET acquisition lasts slightly longer than the irradiation [4]. This may mismatch the constraint of a medical center and make real-time monitoring impossible with such a device.

Besides PET, prompt-γ radiation detection may be regarded as a promising technique to control the dose during ion irradiation treatments. Indeed, within less than a nanosecond following the ion beam impact, γ and neutrons are emitted by excited nuclei each time nuclear fragmentation occurs with high probability. Moreover, the longitudinal distribution (along the beam direction) of the prompt radiation emission is tightly correlated to the primary beam range, since fragmentation occurs all along the ion path. Thus, we can deduce in principle the dose distribution from prompt radiation measurements. Technically, this requires to design an imaging device with a physical or electronic collimation that is able to discriminate radiations coming directly from the ion track from those scattered in the surrounding matter, namely elastically- and inelastically-scattered neutrons and Compton-scattered gamma-rays. Recently, Min *et al.* have studied the longitudinal distribution profile of prompt gammas due to the target nuclei fragmentation induced by proton impact on thick targets, using a collimated scanner detection setup. They found that the information on the ion range is kept even for proton energies up to 200 MeV [5].

In the present study we propose to extend this work to carbon ion beams, for which not only target nuclei fragmentation, but also projectile fragmentation takes place, and to improve the detection technique by using combined time-of-flight and energy discrimination techniques. Part of this study has been very recently presented in a letter [6]. This paper presents complementary results, in particular, the dependence of gamma ray and neutron detection yields as a function of the detection angle. In parallel to our experiments, we have developed simulations using the GEANT4 package (version 9.1) [7]. The aim of these simulations is both to improve and validate the input data of the physics list used in the code, and to optimize the experimental setup.

In order to introduce our physics case, we present in Figure 1 the calculated energy and time distributions of neutrons and gammas produced during the irradiation of a PMMA ($C_5H_8O_2$) target by 73 MeV/u carbon ions that are those we used in our experiment. At this energy, 9% of the incident ions undergo inelastic nuclear collisions before stopping. The number of gamma-rays and neutrons emitted per reaction are close to 2 and 3, respectively. As shown in Fig. 1-a, the energy spectrum of gamma rays ranges from zero to more than 20 MeV. This spectrum is composed of discrete peaks, and of a continuum corresponding to gammas emitted before equilibrium is reached in highly excited nuclear matter [8, 9]. The neutrons present a much wider energy spectrum due the varying kinetic energy of fragments. Although the numbers given above are rough, they show that the prompt radiation multiplicity should be high enough to allow the online monitoring of the dose with collimated detectors. Fig.1-b shows the time distribution of the energy deposition in a detector located at 60 cm, perpendicularly to the beam direction (the time scale originates at the time of ion impact on the target). At such a distance, the flight length is large enough to allow a clear separation between gammas and high-energy neutrons (travelling at ~1/3 of the speed of light) with fast scintillation detectors.

II. Experimental set-up

The experiment, performed at the GANIL facility (Caen, France), used a pulsed beam of 73 MeV/u $^{13}C^{6+}$ ions (beam pulses of ~1ns every 80 ns). The fragmentation cross sections and the gamma emission yields of $^{13}C^{6+}$ and $^{12}C^{6+}$ ions are the same within 10%. The additional neutron of $^{13}C^{6+}$ ions leads to slightly larger neutron emission yields. The beam intensity on the target was set to about 1 nA in order to optimize the counting rate on the detectors. Figure 2 shows a picture of the detection set-up. The beam, extracted in air from the vacuum beamline, impinged on a PMMA cubic shaped target set on a table allowing its translation along the beam direction by means of a remote control system. We used two targets with different side lengths, 5 and 15 cm; the results correspond to measurements performed with the latter target.

The main detector, a cylindrical NaI detector 5cm in diameter and length, was placed at a distance from the target varying from 45 cm to 95 cm, depending on the collimation set-up. The collimation configurations used are summarized as follows: a 20 cm thick lead collimator, with an adjustable slit width (from 1 to 4 mm) was set at a detection angle θ=120°(backward direction), 90° and 60° (forward direction) with respect to the beam direction. An additional paraffin collimation system could be added.

The dose was monitored by means of a second NaI detector placed at a larger distance in order to get a counting rate proportional to the beam intensity, nearly independently of the target position and collimation. This monitor was calibrated with a Faraday cup at higher intensities.

The detector readout (time and energy distributions) was performed with a conventional nuclear electronics, namely NIM shaping amplifiers and logic and a VME data acquisition. A key point of our experiment was the discrimination between detected gamma rays and neutrons by the time-of-flight technique (TOF): the difference T between the detection time by the scintillator and a given phase of the RF-signal from the accelerator was treated by a TAC (Time to Analogical Converter). Finally, the data recorded were the energy deposited E and the time T associated to each detection event, along with the number of counts N detected by the dose monitor during a run.

The main parameters of our experimental set-up were the following: i) the target-to-main detector distance and the detection angle θ ii) the collimator slit width iii) the presence or not of an additional paraffin shielding against neutrons and, iv) off-line, the selection of the detected radiations as a function of the energy deposited in the detector and of their time-of-flight. Concerning the geometrical parameters, the target-to-main detector distance and the collimator slit were set to 60 cm and 2 mm, respectively, the additional shielding against neutrons turned out to be useless thanks to the TOF technique.

III. Results

Figure 3 shows a two-dimensional spectrum of the γ-equivalent energy deposited E in the collimated scintillator as a function of the time of flight TOF when the detector aims at a location at the middle of the ion path (with a detection angle θ=90°). The quantity "γ-equivalent energy deposited" refers to the fact that the detector calibration has been performed with a gamma radioactive source, knowing that the luminescence yield of neutrons is different from the gamma one.

As expected, most of the 2D spectrum is dominated by neutrons with a broad time-of-flight spectrum at γ-equivalent energy E lower than 1 MeV. A prompt γ-ray peak appears

nicely around the origin of the time scale even though the time resolution is not as good as expected because of electronic tuning problems (and thus the inverse-comma shape is meaningless).This prompt peak completely disappears when the detector aims at a location beyond the Bragg peak region. The fact that photon detection with E<1 MeV is completely overwhelmed by the neutron background imposes to perform a double selection in energy and time of flight to isolate prompt γ-rays. The rectangle on Figure 3 shows the selection we have chosen: E>1 MeV and -3 ns <TOF<3 ns.

Let us consider a monodimensional portion of the previous bidimensional spectrum to obtain the time of flight spectrum with a selection E>1 MeV. This time of flight spectrum (measured with a detection angle θ=90°) is presented in Figure 4 along with two other spectra measured at θ=120° and θ=60°. We also plotted the gamma-ray component obtained after subtraction of a background spectrum in the measured spectra (the background is measured beyond the ion path at about z=25 mm). As expected, the neutron component decreases with the angle θ of detection: for θ=60° (forward angle), it is about twice the rate measured at 90° and three times the rate measured at 120°. Indeed, as the neutron momentum mainly comes from the momentum of the incident projectile, neutrons are emitted preferentially at forward angles. Moreover, the maximum of the neutron time distribution increases with the angle of detection: the larger the neutron emission angle, the lower their mean kinetic energy. Concerning photons, the rates measured at θ=120° and 60° can be considered as equal within the experimental uncertainties. The rate obtained at 90° is slightly smaller, although we cannot conclude in a significant anisotropy at this stage (part of this effect can be attributed to an increase of the field of view when the detector is moved away from the detection angle θ=90°). Therefore, the signal-to-background ratio is slightly better at backward angles which could be taken advantage of for the design of a prototype to improve the discrimination between γ-rays and fast neutrons, in particular with high energy beams.

For the present work, we used a detection angle θ=90° to measure the detection rate profile as a function of the longitudinal position z. Figure 5 shows gamma and neutron profiles (corresponding to TOF>10 ns) in connection with a scaled picture of the PMMA target after irradiation. Thanks to the high dose delivered to the target (>10^5 Gy), the damaged zone was darkened, allowing a precise determination of the ion range: 14 mm. The comparison of the γ-ray profile with the darkened area extension clearly shows that this profile is strongly correlated to the ion path in the target. On the contrary, the neutron yield slowly increases as a function of the position z because neutrons are not filtered by the lead collimator and they are mostly emitted toward forward angles.

One may be surprised by the enhancement of the γ-ray yield observed when the detector aims at the Bragg peak location. This can be partly attributed to a possible increase of fragmentation cross sections when the ion energy decreases [10]. However, the narrowness of this enhancement can be more probably explained by the effect of relatively long radiative decay times of excited fragments. With radiative decay times of the order of the path duration of the ion in the target (*i.e.* a few tens of picoseconds), such a yield enhancement could be reproduced by preliminary simulations.

IV. Discussion

The crucial features of the γ-ray profile (namely the spatial resolution and the detection rates) meet the requirements of an on-line monitor for ion therapy. Indeed, with a signal-to-background ratio of about 3 at the Bragg peak location, the ion range can be determined with an accuracy of about 1 mm. And we do observe about 10^{-7} prompt gamma

per incident ion with a single 5cm in diameter, 5 cm thick NaI(Tl) detector located at 60 cm and through a 2 mm-wide collimation. This yield can be increased by typically 3 orders of magnitude by improving : i) the geometrical efficiency by more than 2 orders of magnitude thanks to the TOF technique that makes it possible to reduce the radiation shielding to the minimum and to increase the number of detectors, ii) the intrinsic efficiency, with either larger NaI(Tl) scintillator or other detectors such as BaF_2. We can therefore expect a yield of 10^{-4} prompt γ-ray to be multiplied by the 10^6 - 10^7 ions required for the treatment of a 1 cm^3 tumor within one session [11]. Thus online control with prompt radiation is realistic. Moreover, optimization of the signal-to-background ratio can be obtained if necessary by improving the time resolution of the gamma detector.

Developments are in progress to improve our dose monitoring technique. Some of them will be necessary to obtain a device that meets the requirements of hadrontherapy dose monitoring with the kind of ion beams used for carbon ion irradiation, namely high energy, non-pulsed ion beams delivered by synchrotrons. Indeed, at high energies, we expect a larger neutron background and non-pulsed ion beams imply that the time reference for the TOF technique has to be provided by a fast detector intercepting the beam. These developments will hopefully be available for our next beam time at GSI to validate our dose monitoring technique with a typical hadrontherapy beam.

Within the frame of the French Pôle National de Recherche en Hadrontherapie, the Research groupment GDR MI2B, supported by the French CNRS, and the ETOILE center for Hadrontherapy, supported by the Rhône Alpes Region, further studies are now undertaken to improve this dose monitoring technique.

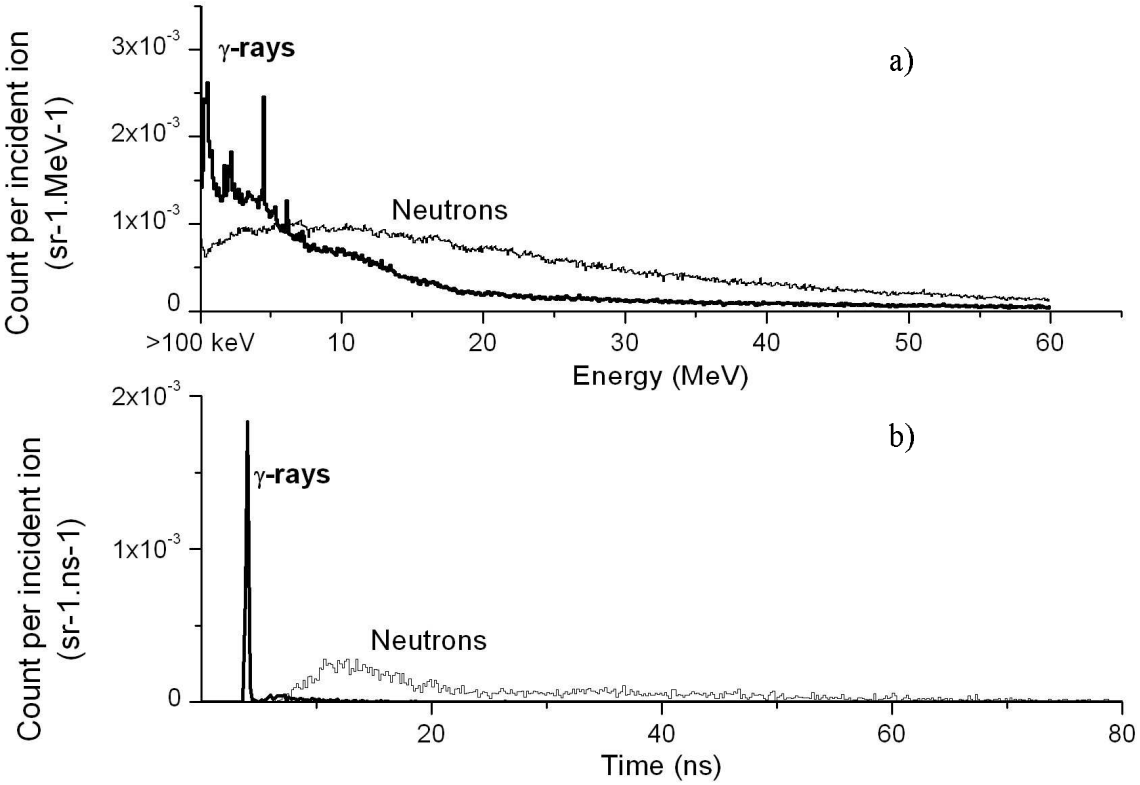

Figure 1. a) Energy spectra of gamma rays and neutrons produced by nuclear fragmentation of 73 MeV/u carbon ions on a PMMA target (Geant4 simulation). b) Simulated time distribution of the energy deposited in a detector positioned at 60 cm from the target with a collimator slit of 2 mm

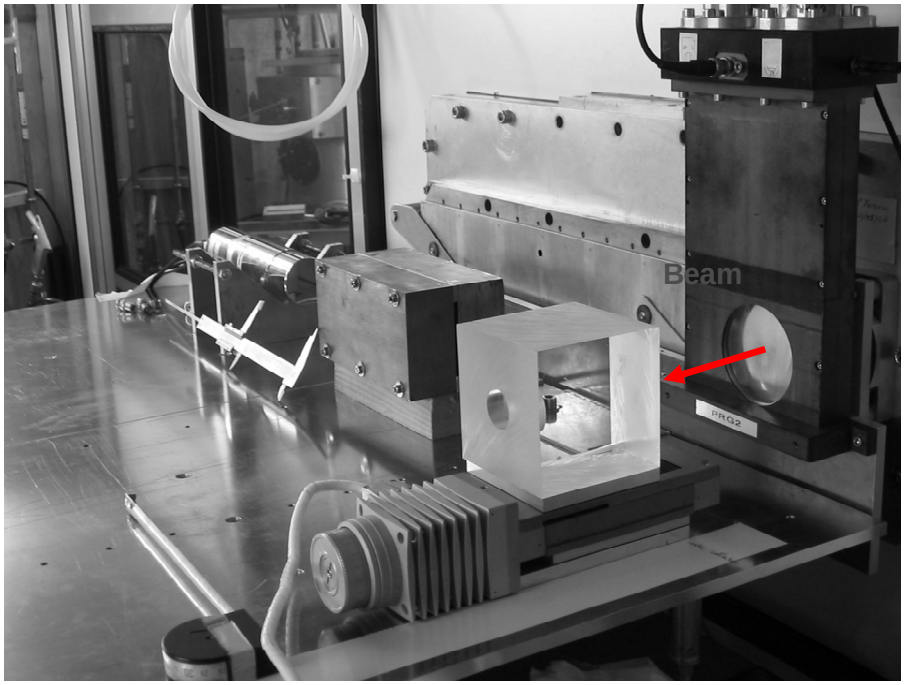

Figure 2. Picture of the experimental set-up with a target-to-main detector distance set to 60 cm and a detection angle θ=90° (with respect to the beam direction)

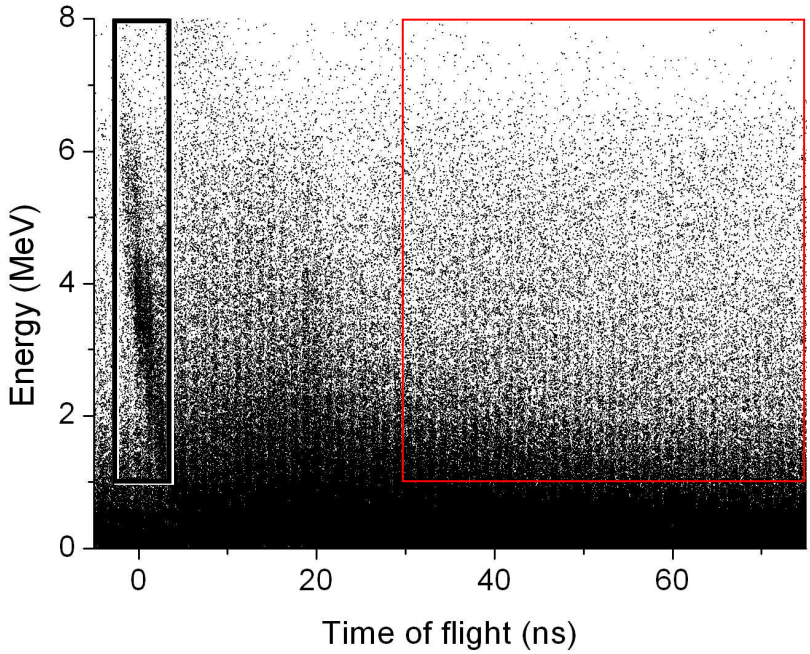

Figure 3. Two-dimensional spectrum of the γ-equivalent energy deposited E in the collimated scintillator as a function of the time of flight TOF when the detector aims at a location at the middle of the ion path (with a detection angle θ=90°). The left rectangle corresponds to the selection of prompt γ-rays we have chosen, and the right one to a neutron selection.

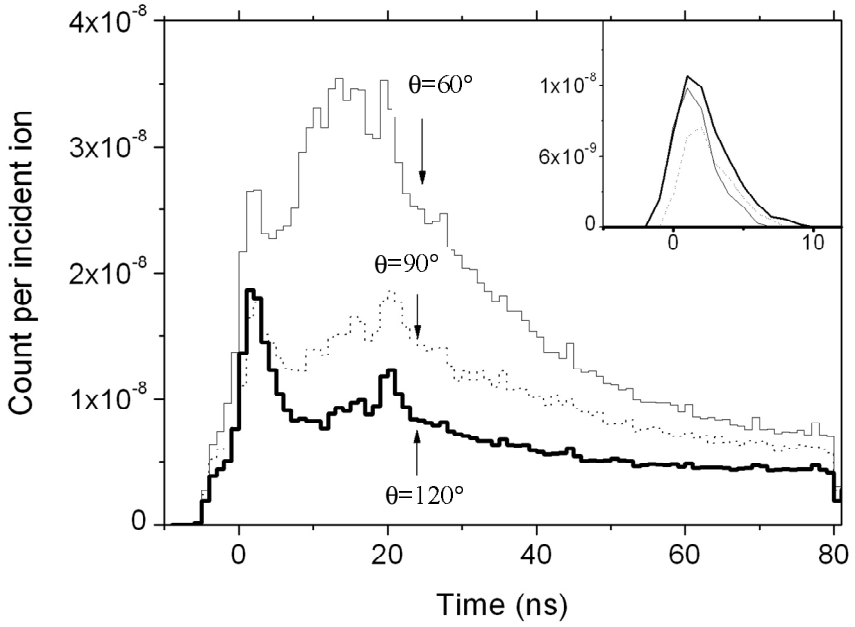

Figure 4. Time-of-flight spectra measured at three detection angles (θ=120°, 90° and 60°) for a longitudinal position z=8 mm and a selection on the energy deposited E>1 MeV. The inset corresponds to the time-of-flight spectrum of the photons obtained after subtraction of a background TOF spectrum (recorded at *z*=25 mm)

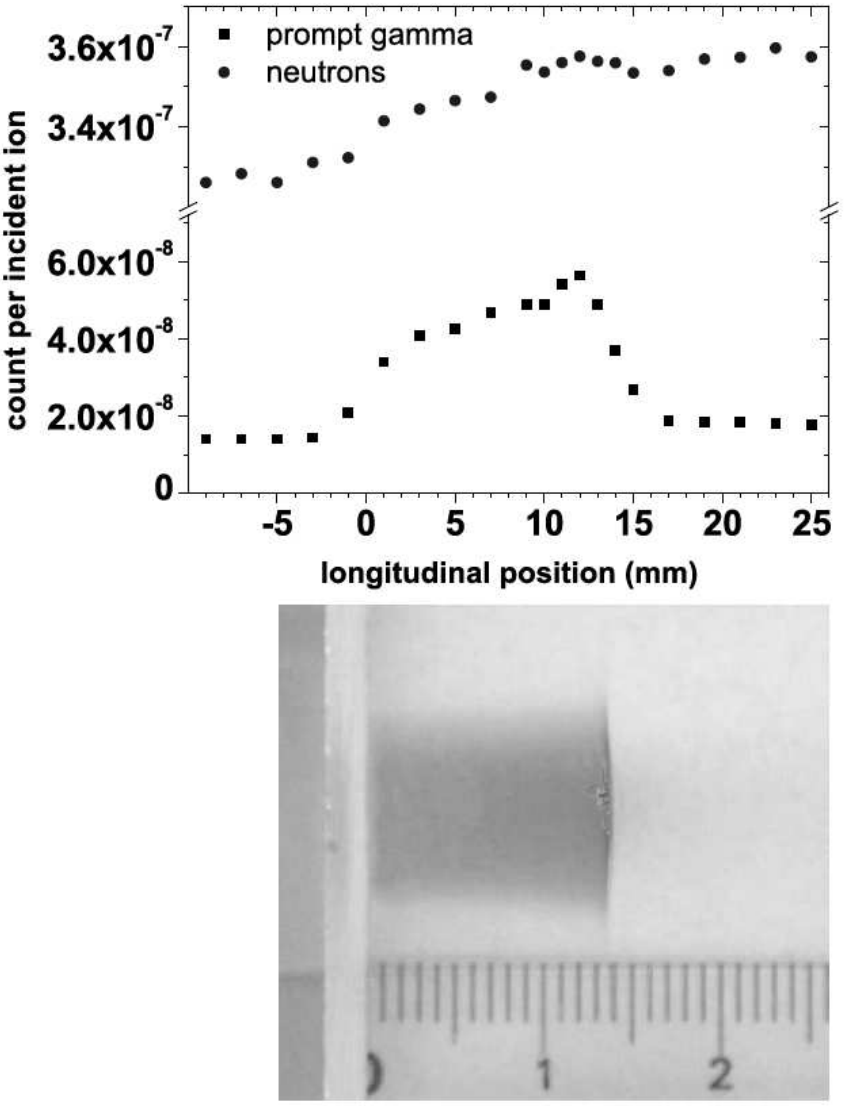

Figure 5. Detection rates as a function of the longitudinal position z obtained for the two different selections on the time of flight TOF and the energy deposited E in the detector indicated in Figure 3: photon selection (square symbols) and neutron selection (circle symbols).

References

[1] U. Amaldi and G. Kraft, Rep. Prog. Phys. 68 (2005) 1861

[2] I. Shall, D. Schardt, H. Geissel, H. Irnich, E. Kankeleit, G. Kraft, A. Magel, M.F. Mohar, G. Münzenberg, F. Nickel, C. Scheidenberger, and W. Schwab, Nucl. Instr. And Meth. B, 117 (1996) 221

[3] P. Crespo, Optimization of In-Beam Positron Emission Tomography for Monitoring Heavy Ion Tumor Therapy, Dissertation:TU Darmstadt, Fachbereich Physik, 2005

[4] J. Pawelke, T. Bortfeld, F. Fiedler, T. Kluge, D. Möckel, K. Parodi, F. Pönisch, G. Shakirin, and W. Enghardt, IBIBAM proceedings (2007) 97

[5] C.-H. Min, C. H. Kim, M.-Y. Youn, and J.-W. Kim, Appl. Phys. Lett., 89 (2006) 183517

[6] E. Testa, M. Bajard, M. Chevallier, D. Dauvergne, F. Le Foulher, N. Freud, J.-M. Létang, J.-C. Poizat, C. Ray, and M. Testa, Appl. Phys. Lett. 93 (2008) 093506

[7] S. Agostinelli *et. al.* (GEANT4 Collaboration), Nucl.Instrum. Methods A, 506 (2003) 250-303

[8] G. Martínez, F.M. Marqués, Y. Schutz, Gy. Wolf, J. Díaz, M. Franke, S. Hlaváč, R. Holzmann, P. Lautridou, F. Lefèvre, H. Löhner, A. Marín, T. Matulewicz, W. Mittig, R.W. Ostendorf, J.H.G. van Pol, J. Québert, P. Roussel-Chomaz, A. Schubert, R.H. Siemssen, R.S. Simon, Z. Sujkowski, V. Wagner, and H.W. Wilschut, Phys. Lett. B 349 (1995) 23

[9] H Nifenecker and J A Pinston, Annu. Rev. Nucl. Part. Sci., 40 (1990) 113-144

[10] W-Q Shen, B Wang, J Feng, W-L Zhan, Y-T Zhu and E-P Feng, Nucl. Phys. A 491 (1989) 130

[11] D. Schardt and the Heavy-Ion Therapy Collaboration, Nucl. Phys. A. 787, (2007) 633c